Chemical Physics 398 (2012) 206–213

Contents lists available at ScienceDirect

Chemical Physics

journal homepage: www.elsevier.com/locate/chemphys

Dissociative electron attachment to vibrationally excited H_2 molecules involving the $^2\Sigma_g^+$ resonant Rydberg electronic state

R. Celiberto [a,b,*], R.K. Janev [c,d], J.M. Wadehra [e], J. Tennyson [f]

[a] Department of Water Engineering and Chemistry, Polytechnic of Bari, 70125 Bari, Italy
[b] Institute of Inorganic Methodologies and Plasmas, CNR, 70125 Bari, Italy
[c] Macedonian Academy of Sciences and Arts, P.O.B 428, 1000 Skopje, Macedonia
[d] Institute of Energy and Climate Research – Plasma Physics, Forschungszentrum Jülich GmbH Association EURATOM-FZJ, Partner in Trilateral Euregio Cluster, 52425 Jülich, Germany
[e] Physics Department, Wayne State University, Detroit, MI 48202, USA
[f] Department of Physics and Astronomy, University College London, London WC1E 6BT, UK

ARTICLE INFO

Article history:
Available online 14 May 2011

Keywords:
Dissociative attachment
Rydberg states
Vibrationally excited molecules

ABSTRACT

Dissociative electron attachment cross sections (DEA) on vibrationally excited H_2 molecule taking place *via* the $^2\Sigma_g^+$ Rydberg-excited resonant state are studied using the local complex potential (LCP) model for resonant collisions. The cross sections are calculated for all initial vibrational levels ($v_i = 0$–14) of the neutral molecule. In contrast to the previously noted dramatic increase in the DEA cross sections with increasing v_i, when the process proceeds *via* the $X\,^2\Sigma_u^+$ shape resonance of H_2, for the $^2\Sigma_g^+$ Rydberg resonance the cross sections increase only gradually up to $v_i = 3$ and then decrease. Moreover, the cross sections for $v_i \geqslant 6$ exhibit pronounced oscillatory structures. A discussion of the origin of the observed behavior of calculated cross sections is given. The DEA rate coefficients for all v_i levels are also calculated in the 0.5–1000 eV temperature range.

1. Introduction

The dissociative electron attachment (DEA) process for molecules plays a decisive role in many hydrogen plasmas. The importance of DEA in the negative ion sources, for instance, is well known; in these sources, the production of the H^- species comes mainly from dissociative attachment to vibrationally excited H_2 molecule, and the formation of these ions is dramatically enhanced if the nuclear modes of the molecules are highly excited [1,2]. In general, the DEA process plays a significant role in all non-equilibrium hydrogen plasmas, in which a strong non-Boltzmann distribution generates a high density of vibrationally and rotationally excited H_2 molecules. The divertor region in thermonuclear fusion devices [3] and the physical environment of the early Universe [4] provide further examples of such plasma/gas conditions.

Among the various theoretical approaches to the resonant electron–molecule collisions [5–10], a proper description of DEA and related processes (such as the resonant vibrational excitation) is provided by the nonlocal resonance theory. This theory is usually formulated using the projection-operator formalism and leads to an integro-differential equation for the nuclear motion, involving the coupling of discrete and continuum electronic states of the resonant system. This coupling is accounted for by the nonlocal coupling matrix of the electronic Hamiltonian, $V(\epsilon, R) = \langle \Phi_d | \mathbf{H}_{el} | \Psi_\epsilon \rangle$, expressed in terms of the discrete and continuum electronic wave functions, Φ_d and Ψ_ϵ, which both parametrically depend, within the Born–Oppenheimer approximation, on the internuclear separation R. The coupling matrix derives the attribute *nonlocal* from its dependence on the continuum electron energy, ϵ, which gives rise to a complex, energy-dependent, nonlocal potential in the equation for the nuclear motion [11,12].

If certain physical conditions are fulfilled, the energy dependence of the coupling matrix can be suppressed, and an approximate *local* differential equation for the nuclear motion is obtained. This happens, for example, when the real part of the potential energy curve of the resonant state is well separated from that of the neutral molecule involved in the collision. This implies high energy-threshold values for the process and, consequently, high incident electron energies. Under these conditions, the rovibrational spacing of the neutral molecule can be considered as negligible, with respect to the incident electron energy, and the collapse of the nuclear eigenvalues, to certain suitable selected value can be assumed. The coupling matrix then no longer depends on the incident electron energy and a local complex potential (LCP) arises from the assumption of rovibrational degeneracy.

This situation occurs in the e–H_2 collision system when the incident electron is temporarily captured to H_2 and forms a Feshbach

* Corresponding author at: Department of Water Engineering and Chemistry, Polytechnic of Bari, 70125 Bari, Italy. Tel.: +39 080 5963570.
E-mail addresses: r.celiberto@poliba.it (R. Celiberto), r.janev@fz-juelich.de (R.K. Janev), wadehra@wayne.edu (J.M. Wadehra), j.tennyson@ucl.ac.uk (J. Tennyson).

0301-0104/$ - see front matter © 2011 Elsevier B.V. All rights reserved.
doi:10.1016/j.chemphys.2011.05.004

resonance associated with the Rydberg-excited $^2\Sigma_g^+$ electronic state of the molecular ion. The processes associated with the formation of this resonance,

$$H_2\left(X^1\Sigma_g^+\right) + e \rightarrow H_2^-\left(^2\Sigma_g^+\right) \rightarrow \text{exit channels} \quad (1)$$

have been studied experimentally and theoretically, and cross sections for the vibrational excitation and dissociative attachment channels obtained. Measurements have been performed by Comer and Read [13] who reported vibrational excitation cross sections, along with precious information on potential curves and widths, for several resonance series. The vibrational exit channel, for process (1) were labeled series "*a*". The $^2\Sigma_g^+$ quasi-stable state, which is characterized by a small autodetachment width, was also identified by the same authors as a Feshbach resonance, energetically lying above the excitation thresholds of the first few bound excited molecular states. The theoretical counterpart of the Comer and Read's work, was provided by Stibbe and Tennyson [14], who, using the R-matrix method [15], obtained potential curves and local widths for numerous resonances arising in the $H_2 + e$ system. In particular, the Rydberg $^2\Sigma_g^+$ resonance involved in processes (1), gave vibrational structures in agreement with the experimental measurements of Comer and Read and explained the seemingly contradictory measurements on the isotopically substituted systems [16]. These calculations underpinned the theoretical evaluation of the resonant vibrational cross sections for processes (1), in the frame of the LCP model, which were found to be in excellent agreement with the Comer and Read experiments [17,18].

Cross sections for dissociative electron attachment (DEA) were measured by Schulz [19] and Rapp et al. [20], who observed two peaks at electron energies of 10 and 14 eV. The first maximum was assumed to be generated by the B $^2\Sigma_g^+$ resonant excited state of the H_2^- anion, which can be associated with the repulsive parent state b $^3\Sigma_u^+$ of the H_2 molecule. The second, and the largest peak, was ascribed to a resonant state, of Rydberg nature, which dissociates to an $n = 2$ excited H atom besides the H^- negative ion [21,22]. However the magnitude of this, the stronger peak, differed between the two measurements by more than the experimental errors. Assuming that this state is the one identified by Comer and Read as responsible for series *a*, Celiberto et al. [23] calculated the LCP dissociative attachment cross sections for the 14 eV process which were found to be in striking agreement with Schulz's measurements. Although these results cannot be considered definitive in confirming Schulz's cross sections [19], they showed, together with the good results achieved for the vibrational excitation discussed above, the reliability of the LCP model in describing realistically the collision processes occurring through the $^2\Sigma_g^+$ Rydberg resonance.

In the present work we extend the application of the LCP method to study the DEA processes from vibrationally excited H_2 molecules, namely

$$H_2\left(X^1\Sigma_g^+, v_i\right) + e \rightarrow H_2^-\left(^2\Sigma_g^+\right) \rightarrow H(n=2) + H^-(1s^2) \quad (2)$$

and calculate the DEA cross sections for all $v_i = 1$–14 for a wide range of electron energies. The corresponding rate coefficients, important in plasma modeling and diagnostic, have been also calculated in the temperature range from about 0.5 to 1000 eV.

In the next section we summarize the main points of the resonant theory, while the results are presented and discussed in Section 3. In Section 4 we give our conclusions.

2. Theoretical model

In this section only a brief account is given of the concepts and relevant equations of the theory of electron–molecule resonant processes. For a deeper insight in the subject, the reader is directed to the previous literature [5,6,17,22].

A molecular resonant state can be described as an overlap of a discrete state, formed by the extra electron captured by the target molecule, with the continuum states where the electron acts as an unbound particle. The scattering wave function can then be written, within the Born–Oppenheimer approximation, as

$$\Psi = \Phi_d(\mathbf{r}_i; R) + \sum_{vJ} \int_0^\infty d\epsilon f_{vJ}(\epsilon)\psi_\epsilon(\mathbf{r}_i; R)\chi_{vJ}(\mathbf{R}) \quad (3)$$

where $\Phi_d(\mathbf{r}_i; R)$ and $\psi_\epsilon(\mathbf{r}_i; R)$ are the discrete and continuum wave functions respectively, both of which depend on the electron position vectors, collectively denoted by $\mathbf{r}_i$, and parametrically on the internuclear distance R. ϵ is the continuum energy, $f_{vJ}(\epsilon)$ is a linear combination coefficient, and $\chi_{vJ}(\mathbf{R})$ is the rovibrational wave function of the target molecule. The sum runs over the bound and continuum rovibrational levels. Substitution of Eq. (3) in the Schrödinger equation leads to the nonlocal integral equation of the form [17]:

$$\left[-\frac{\hbar^2}{2M}\frac{d^2}{dR^2} + \frac{\hbar^2 J_i(J_i+1)}{2MR^2} + V^-(R) - E\right]\xi_i(R) = -f(\epsilon_i)F_i(R)\chi_{v_iJ_i}(R) - \sum_{vJ} c_{vJ}F(R)\chi_{vJ}(R) \times \int_0^\infty dR'\chi^*_{vJ}(R')F^*(R')\xi_i(R') \quad (4)$$

where the coupling matrix has been factorized as a product of two functions respectively dependent on the energy and on the internuclear distance:

$$V(\epsilon, R) = f(\epsilon)\cdot F(R) \quad (5)$$

The matrix element $V(\epsilon_i, R) = f(\epsilon_i)\cdot F_i(R)$ is known as the entry amplitude and describes the capture of the incoming electron, with kinetic energy ϵ_i, by the target molecule, assumed here in its ground electronic state $X\ ^1\Sigma_g^+$. The coupling matrix element, in general, is related to the resonance nonlocal width by the expression

$$\Gamma(\epsilon, R) = 2\pi|V(\epsilon, R)|^2 = 2\pi|f(\epsilon)\cdot F(R)|^2 \quad (6)$$

$\xi_i(R)$, in Eq. (4), is the resonant nuclear wave function, with the subscript i denoting the initial rotational state J_i. $V^-(R)$ is the adiabatic potential of the resonant state, and $\chi_{vJ}(R)$ is the radial rovibrational target wave function. The coefficient c_{vJ_i} is given by

$$c_{vJ_i} = P\int_0^\infty d\epsilon \frac{|f(\epsilon)|^2}{\epsilon_{vJ_i} - \epsilon} - i\pi|f(\epsilon_{vJ_i})|^2 \quad (7)$$

Here P denotes the principal value of the integral and ϵ_{vJ_i} is defined by $\epsilon_{vJ_i} = E - E_{vJ_i}$, where E is the total energy end E_{vJ_i} the molecular energy eigenvalues.

In the present work Eq. (4), for process (2), has been solved by assuming the local form of the input parameters for the resonant state (i.e. resonance potential and widths) the same as those used in Refs. [17,23] and taken from [14]. In particular, the local resonance width $\Gamma(R) = 2\pi|F(R)|^2$, the partial width $\Gamma_X(R) = 2\pi|F_i(R)|^2$, and the resonance potential $V^-(R)$, in the interval $R = 1.1 - 4.0\ a_0$, were taken from this last reference. The extrapolation of these quantities outside this range has been implemented by adopting suitable analytic functions [17,23]. The dimensionless energy dependent part in Eq. (5) has been put equal to 1, which is consistent with the width being very narrow. Finally, the bound vibrational wave functions $\chi_{vJ_i}(R)$, were obtained by solving the nuclear Schrödinger equation for the H_2 molecule using the potential curve of Kolos and Wolniewicz [24] for the ground electronic state. Fig. 1 gives a representation of the relevant input quantities, namely, the potential energy curves for the resonant and neutral

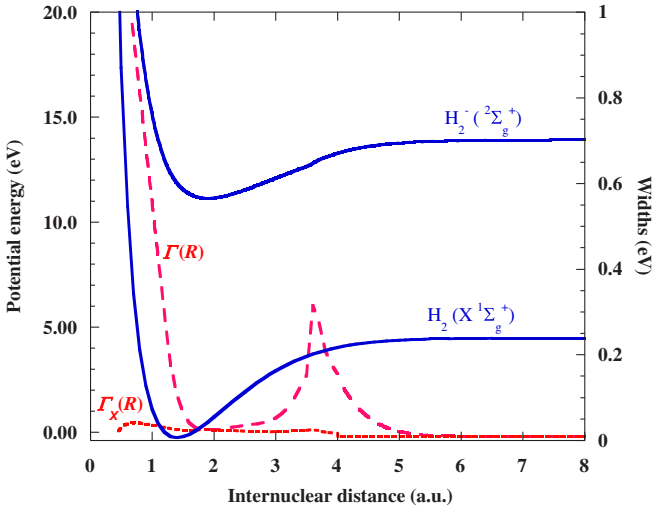

Fig. 1. Potential energies and widths required in the cross section calculations. Full lines: potential energies for the H_2 electronic ground state (lower curve) and H_2^- resonant state (upper curve); dashed lines: total $\Gamma(R)$ (long dashed) and partial $\Gamma_X(R)$ (short dashed) resonance widths.

electronic states respectively (left scale), as well as the total and partial local widths (right scale) as a function of the internuclear distance [17,23]. One of the general features of the widths shown in the figure is that, unlike the well known case of the broad X $^2\Sigma_u^+$ shape resonance, they are characterized by a relatively small magnitude, which is consistent with the long-lived Feshbach nature of the Rydberg state.

Eq. (4) can be cast in local form by applying the degenerate-state approximation, discussed in the introduction, and assuming that the coefficient $c_{v_i J_i}$ is almost constant. In this case, the coefficient $c_{v_i J_i}$ can be carried out of the sum, and making use of the closure relation for the vibrational wave functions, Eq. (4) becomes

$$\left[-\frac{\hbar^2}{2M}\frac{d^2}{dR^2}+\frac{\hbar^2 J_i(J_i+1)}{2MR^2}+V^-(R)+\Delta(R)-\frac{i}{2}\Gamma(R)-E\right]\xi_i(R) = -F_i(R)\chi_{v_i J_i}(R) \tag{8}$$

where the *level shift*, $\Delta(R)$, is given by

$$\Delta(R) = |F(R)|^2 \cdot P\int_0^\infty d\epsilon \frac{|f(\epsilon)|^2}{\epsilon_{\bar{v}J_i}-\epsilon} \tag{9}$$

and the energy width $\Gamma(R)$ is given by Eq. (6) with $f(\epsilon)=1$. The quantum numbers $\bar{v}$,J_i, in the above equation, indicate a selected rovibrational state, representative of the whole manifold of the rovibrational levels. However, in the present calculations, following an often adopted approximation [17,23,25,26], the level shift has been included in the anion potential $V^-(R)$.

Although the input parameters were provided in local form [14], in this work we actually used the nonlocal equation in its general form (4); as discussed below, we used the local Eq. (8) only to check some particular results. Throughout the paper we will assume $J_i = 0$ and no rotational transitions will be considered.

3. Results

Once the non-local Eq. (4) has been solved, and the nuclear wave function obtained, the DEA cross sections can be calculated from [23]

$$\sigma(\epsilon_i) = 2\pi^2 \frac{m}{M}\frac{K}{k_i}\lim_{R\to\infty}|\xi_i(R)|^2 \tag{10}$$

where m and M are the electron and reduced nuclear masses respectively, K is the relative atom-negative-ion outgoing momentum and k_i the initial momentum corresponding to the incident electron kinetic energy ϵ_i.

The cross sections obtained from Eq. (10), as a function of the incident electron energy, are shown in Figs. 2–6, for each initial vibrational level v_i (indicated in the panel) of the molecule H_2. For ease of comparison, all panels in Figs. 2–6 are constructed with same scale and same range of cross sections and electron energies. The cross section for $v_i = 0$ (Fig. 2), taken from Ref. [23], is also included in this figure for completeness and comparison. Two remarkable features can be observed in the energy behavior of the cross sections shown in Figs. 2–6: (i) the cross section peaks increase with increasing initial vibrational level up to $v_i = 3$ and then start to decrease, and (ii) for $v_i \geqslant 6$ oscillatory structure appears in the cross sections, the number of oscillations increasing with the increase of v_i. This energy behavior is in contrast with the one observed in the case of DEA cross sections in the e–H_2 system when the process is mediated by the X $^2\Sigma_u^+$ shape resonance [1,2,27],

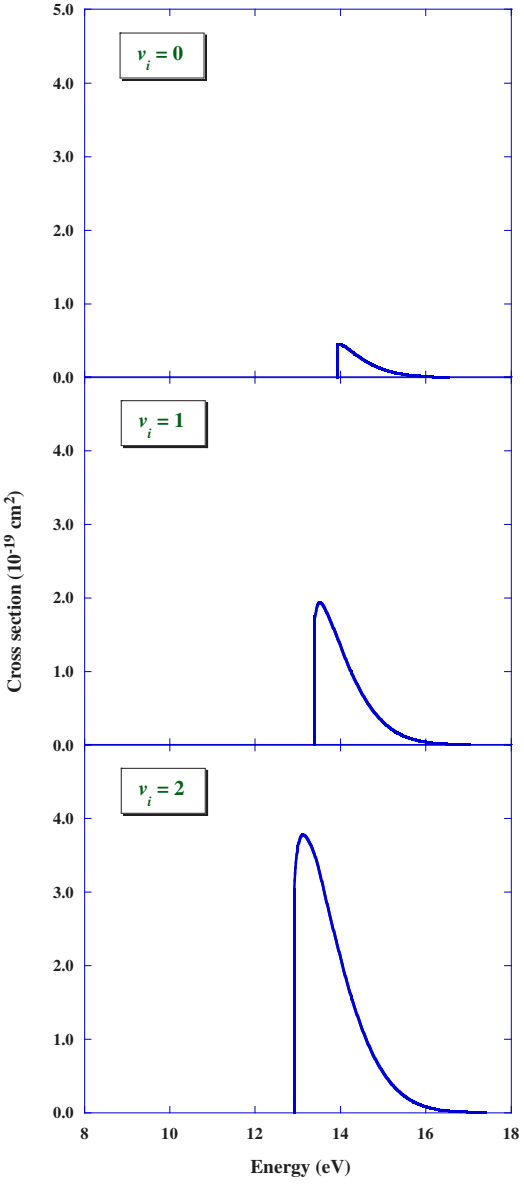

Fig. 2. Cross sections for the DEA process for H_2 starting from the level v_i shown in the figure.

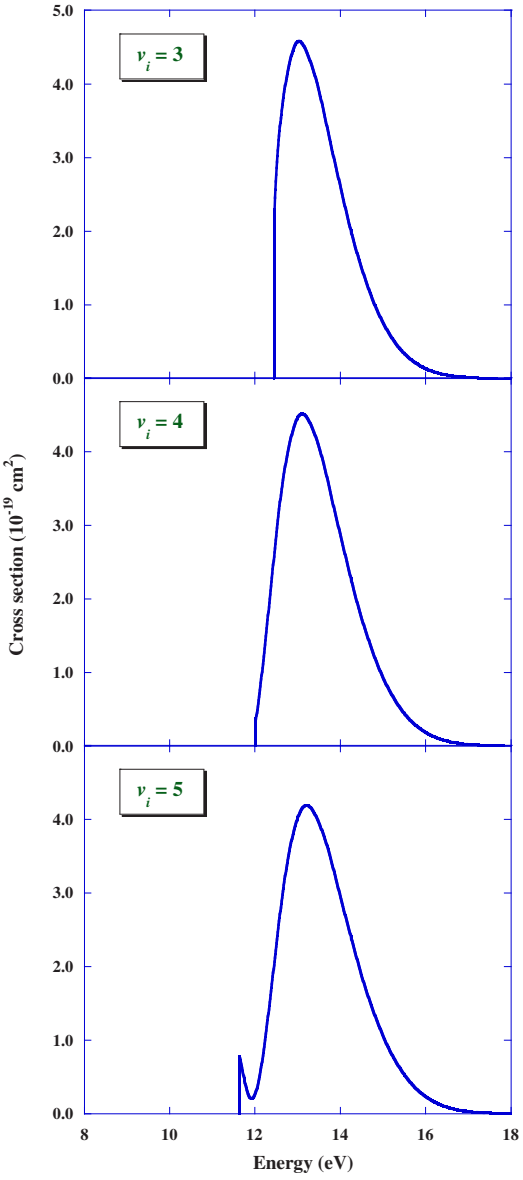

Fig. 3. Cross sections for the DEA process for H_2 starting from the level v_i shown in the figure.

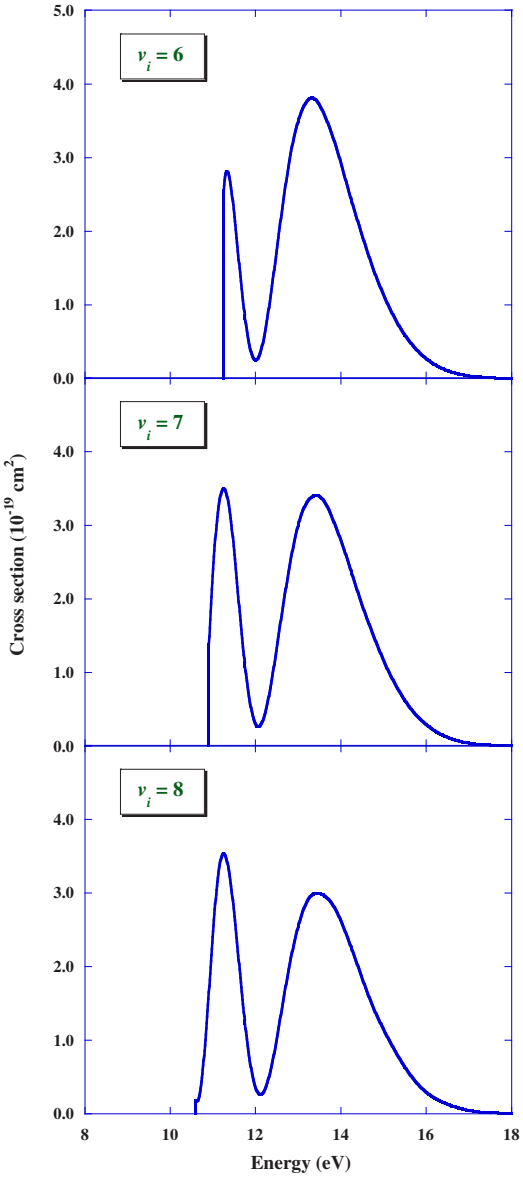

Fig. 4. Cross sections for the DEA process for H_2 starting from the level v_i shown in the figure.

showing a steady and dramatic increase in the cross section peaks when v_i increases with no oscillatory structures. It should be noted that oscillations in the DEA cross sections for higher v_i have previously been predicted (within the LCP model) for the of e–N_2 system [28]. Qualitatively similar oscillatory behavior has been observed also in vibrational-state dependence of the β parameters for resonance enhanced photoionisation of H_2 [29].

In order to check our calculations (performed, as mentioned earlier, using the non-local Eq. (4), but with the local form of parameters of the resonant state), we have solved also the local Eq. (8). As illustrated in Ref. [17], Eq. (4) is solved by utilizing a numerical algorithm based on the calculation of the Green's function by the Numerov method. The corresponding Green's function for Eq. (8) was obtained using the integral method formulated in Ref. [30] (see also Ref. [31]), modified for the appropriate boundary conditions. It was applied to the calculation of the regular and irregular solutions of the homogeneous equation associated to Eq. (8), through which the resonant wave function can be expressed in the form [5]

$$\xi_i(R) = -\frac{1}{W}\cdot\frac{2M}{\hbar^2}\int_0^\infty dR' u_I(R_<)u_{II}(R_>)F_i(R')\chi_{v_i}(R') \tag{11}$$

where $u_I(R)$ and $u_{II}(R)$ are the two solutions and W is their Wronskian. All other relevant quantities, such as the potential curves, widths and molecular wave functions, were the same as those used in Eq. (4). The cross sections from the two calculations were found to be identical.

At the first sight, the oscillatory cross section behavior as a function of the energy would suggest, according to the reflection principle [32], that oscillations in the cross sections are caused by oscillations of the ground state vibrational wave function. This possibility has been mathematically investigated by O'Malley [33], who, after rewriting Eq. (11) in its asymptotic form,

$$\xi_i(R\to\infty) = -\frac{1}{W}\cdot\frac{2M}{\hbar^2}u_{II}(R\to\infty)\int_0^\infty dR' u_I(R')F_i(R')\chi_{v_i}(R') \tag{12}$$

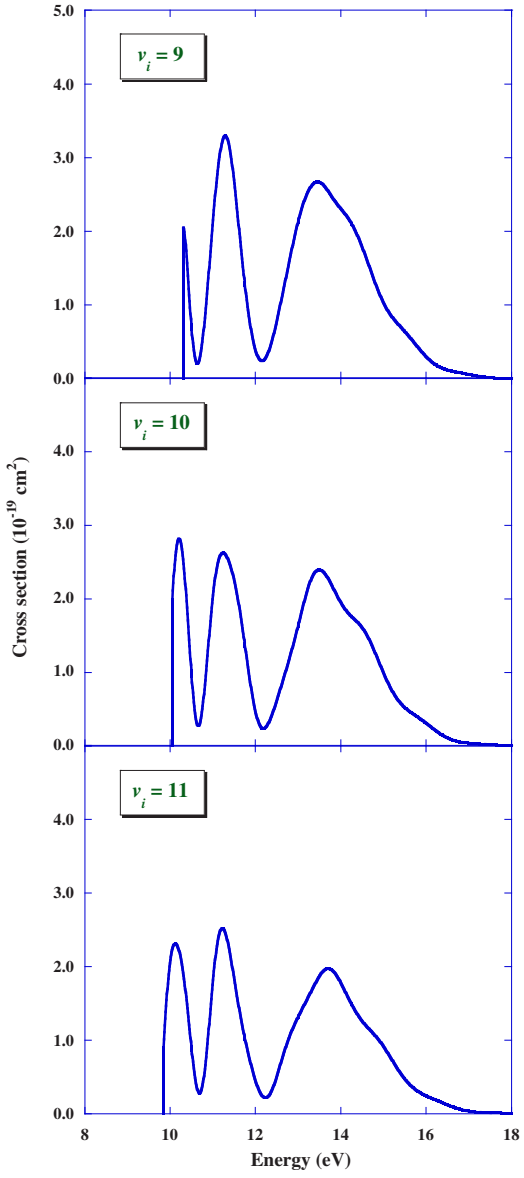

Fig. 5. Cross sections for the DEA process for H_2 starting from the level v_i shown in the figure.

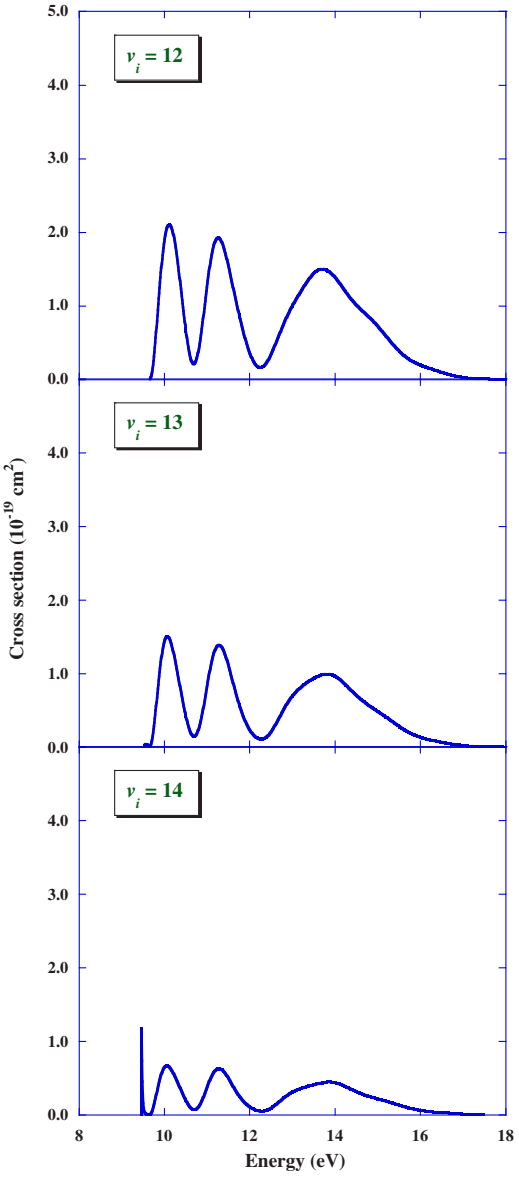

Fig. 6. Cross sections for the DEA process for H_2 starting from the level v_i shown in the figure.

required in Eq. (10), resorted to a semi-classical approximation for the regular part of the Green's function, which was replaced by a δ-function centered at the classical turning point R_c, and showed that the cross sections can be qualitatively expressed as $\sigma(\epsilon_i) \propto |\chi_{v_i}(\alpha R_c - ig)|^2$. Here the imaginary part g equals to the ratio $\Gamma(R_c)/\Gamma_d(R_c)$, where $\Gamma_d = -2V^{-'}(R_c)/\alpha$, $\alpha = (M\omega/\hbar)^{1/2}$ and ω is the harmonic oscillator frequency. To ascertain whether the cross sections follow the behavior of the χ_{v_i}, we have tested the above relation, without the imaginary term ($g \approx 0$), since $\Gamma(R_c)$, for a Feshbach resonance, is small. In fact, an estimate of Γ_d showed that $\Gamma/\Gamma_d \ll 1$ for the repulsive branch of $V^-(R)$, above the DEA threshold where the classical turning points fall. The test has shown that, except for $v_i = 0$, the behavior of $|\chi_{v_i}(R_c)|^2$ does not reproduce the shape of the cross sections, and, for high vibrational levels, not even the number of maxima. This failure of the δ-function approximation shows that the overlap between χ_{v_i} and the regular Green's function in Eq. (12) at the classical turning point is not dominant, and that it covers a wider range of internuclear distances. Therefore, the cross section structure could be produced by the oscillating behavior of the regular Green's function with the energy. In order to verify this possibility we have assumed, for the square of the nuclear wave function of Eq. (10), the approximate form

$$|\xi_i(R \to \infty)|^2 \approx \left|\frac{1}{W}\cdot\frac{2M}{\hbar^2}u_{II}(R \to \infty)F_i(\bar{R})\right|^2 \cdot \left|\int_0^\infty dR' \Psi_v(R')\chi_{v_i}(R')\right|^2 \quad (13)$$

This expression is derived from Eq. (12) by assuming for the entry width a constant value, $F_i(\bar{R})$, and by replacing the complex function $u_I(R)$ by the real continuum wave function $\Psi_v(R)$. This last approximation is justified by the long-lived nature of the Rydberg resonance which, being characterized by small widths, can be considered, to a first approximation, as a true stable state. Assuming thus that $\Gamma(R)$ and $F_i(R)$ are negligibly small, we may rewrite the resonant Eq. (8) as ($J_i = 0$)

$$\left[-\frac{\hbar^2}{2M}\frac{d^2}{dR^2} + V^-(R) - E\right]\Psi_v(R) = 0 \quad (14)$$

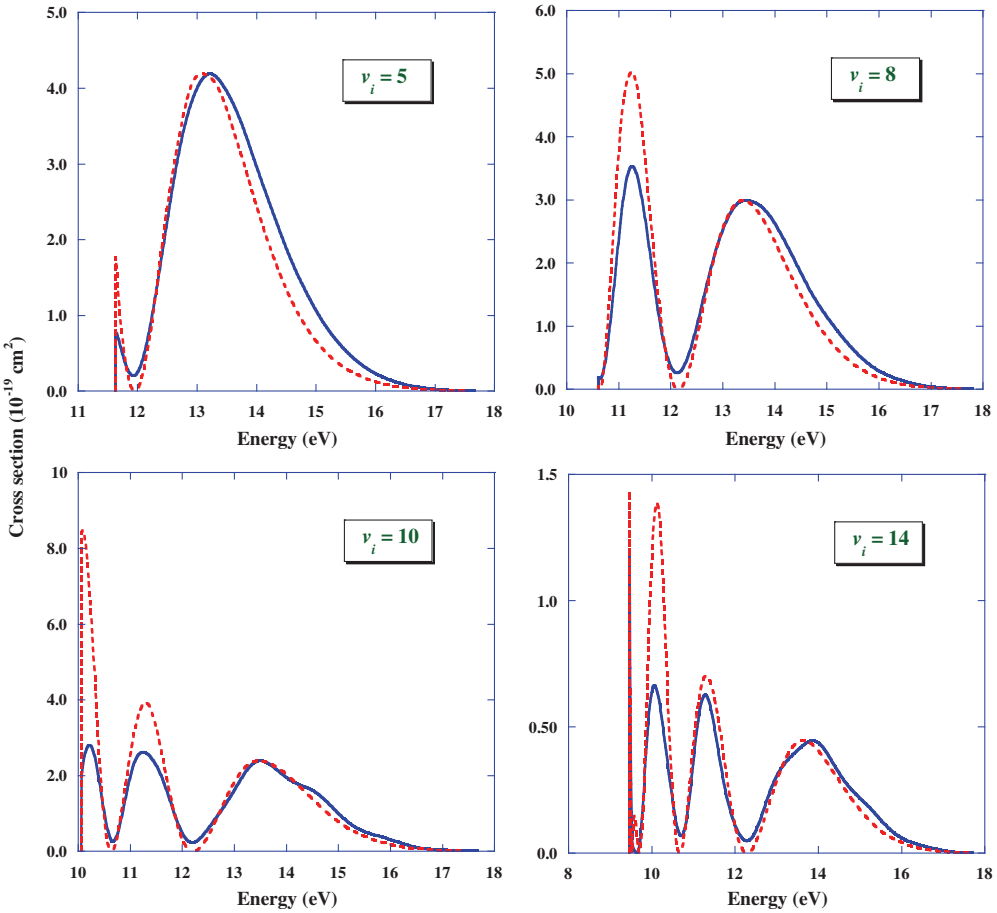

Fig. 7. Squared bound-continuum wave function overlap, $Q_{v_i v}$, (dotted lines) normalized to the highest-energy peak of the calculated DEA cross sections (full lines) as a function of the incident electron energy and for the process starting from the level $v_i = 5$, 8, 10 and 14 shown in various panels.

with the real boundary conditions $\Psi_v(0) = 0$ and $\Psi_v(R \to \infty) \approx K^{-1/2} sin(KR + \eta)$, where η is the phase shift, and $v = \hbar^2 K^2/2M = E - V^-(R \to \infty)$ [30].

After inserting Eq. (13) in Eq. (10), the cross section becomes proportional to the quantity $Q_{v_i v} = \left|\int_0^\infty dR \Psi_v(R)\chi_{v_i}(R)\right|^2$ which can be considered as a Franck–Condon density describing a *dissociative transition* between two stable electronic states. Fig. 7 shows $Q_{v_i v}$ along with the calculated DEA cross sections for the process starting from the vibrational levels $v_i = 5$, 8, 10 and 14, as a function of the incident electron energy. $Q_{v_i v}$ is normalized to the last peak of the DEA cross sections. The qualitative behavior of $Q_{v_i v}$ as a function of the energy, closely following that of the DEA cross section, shows convincingly that the origin of the oscillatory structure in the cross section is the overlap of the initial and final state nuclear wave functions involved in the process.

As mentioned earlier, the DEA cross sections, when the process is mediated by the shape resonance X $^2\Sigma_u^+$, increase dramatically (by many orders of magnitude) as the initial vibrational level increases [1]. This is illustrated in Fig. 8 where the peaks of DEA cross sections, calculated in the present work, are shown as a function of the internal energy of the molecule (the vibrational levels are indicated on the upper scale) and compared with the cross section peaks of the first six levels when the process proceeds *via* the X $^2\Sigma_u^+$ resonance (the latter reduced by a factor of 0.005). We note that the peak of X $^2\Sigma_u^+$ DEA cross section reaches the value of about 10^{-16} cm^2 already for $v_i = 5$ (see Fig. 8) (from its value of $1.65 \cdot 10^{-21}$ cm^2 for $v_i = 0$) and continues to significantly increase with increasing v_i [1,2,27]. The peaks of the present Rydberg $^2\Sigma_g^+$ DEA cross sections are confined to the range $0.5–4.5 \cdot 10^{-19}$ cm^2.

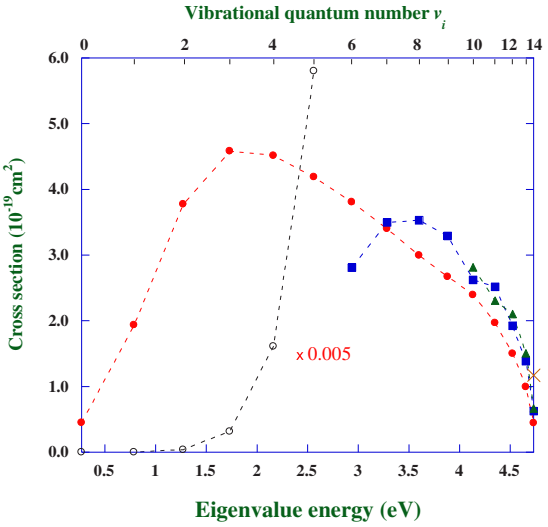

Fig. 8. Peak cross sections as a function of the internal energy (lower scale) of H_2 and of the vibrational quantum number (upper scale). Four series can be identified (see text): I series, filled circles; II series, squares; III series, triangles; IV series, cross. Open circles: X $^2\Sigma_u^+$ shape resonance cross sections reduced by a factor of 1/200.

From a physical point of view, the large difference in the magnitude of cross sections for the two DEA processes can be ascribed to the Feshbach nature of the Rydberg resonance characterized

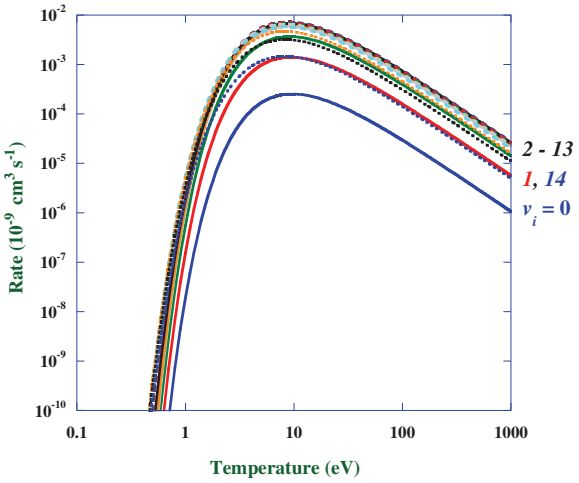

Fig. 9. Rate coefficients as a function of the electron temperature for the DEA processes starting from the v_ith vibrational level of H_2.

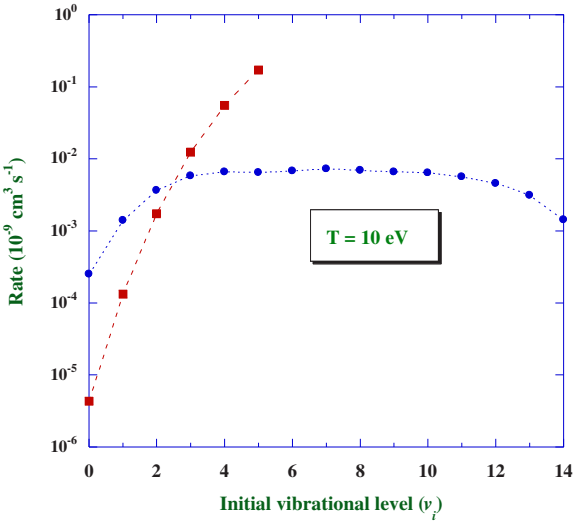

Fig. 10. Rate coefficients as a function of the initial vibrational level of H_2 for electron temperature of 10 eV. Circles: $^2\Sigma_g^+$ Rydberg resonance; squares: X $^2\Sigma_u^+$ shape resonance [34].

by small width, which reduces the inhomogeneous term on the right-hand side of nuclear wave Eq. (8). This term, called entrance probability, is responsible for the generation of the resonance.

Fig. 8 shows also three sets of peaks, corresponding to the three series of peaks observed in the cross sections in Figs. 2–6 as the initial vibrational level v_i increases. The three series start at $v_i = 0,6$ and 10 respectively. A further isolated point appears at $v_i = 14$ (cross), at the process threshold. The series were traced by exploiting the fact that the corresponding peaks for different v_i have similar collision energy, well separated for each set (see the figure caption).

The corresponding attachment rate coefficients, obtained by convolution of the calculated cross sections with a Maxwellian electron energy distribution function, are shown in Fig. 9 as a function of the electron temperature. The rate coefficients attain their maximum values at about $T = 10$ eV and all are confined within a factor of 30. The lowest maximum is for $v_i = 0$ and amounts to $2.5 \cdot 10^{-13}$ cm^3 s^{-1}. It is interesting to note that oscillations in the DEA cross sections for the cases $v_i \geqslant 6$ do not manifest themselves visibly in the rate coefficients. We further note that well below $T = 10$ eV, the rate coefficients decrease exponentially with decreasing T, while well above $T = 10$ eV they decrease as $T^{-3/2}$ with increasing T. This is in accordance with the dependences in these temperature regions established for the rate coefficients of the DEA process proceeding via the X $^2\Sigma_u^+$ shape resonance of H_2 [1,2].

Fig. 10 shows the values of the rate coefficients at $T = 10$ eV for all initial vibrational levels. The distribution of rate coefficients shows a broad plateau between $v_i = 3$ and $v_i = 10$ with a value around $7 \cdot 10^{-12}$ cm^3 s^{-1}. In the same figure we also show the values of rate coefficients at $T = 10$ eV for the first few v_i values when the DEA process proceeds *via* the X $^2\Sigma_u^+$ shape resonance [34]. The comparison shows that for $v_i \leqslant 2$ the rate coefficients for DEA process mediated by the Rydberg $^2\Sigma_g^+$ resonance are larger (by more than an order of magnitude for $v_i = 0,1$) than those when the process is mediated by the X $^2\Sigma_u^+$ shape resonance. This indicates that at plasma temperatures around 10 eV, the DEA in the $e - H_2$ system, leading to H^- ions and H ($n = 2$) excited atoms, can be an important process in the plasma kinetics.

4. Conclusions

We have studied the dissociative attachment of electrons with vibrationally excited H_2 molecules when the process proceeds through the Rydberg-excited $^2\Sigma_g^+$ resonant state. The cross section calculations have been performed within the framework of the LCP model of electron-molecule resonant processes, which for this particular resonant state has already been successfully tested previously [17,23]. With increasing initial vibrational excitation v_i of H_2 the cross section maxima first gradually increase up to $v_i = 3$ and then slowly decrease. For $v_i \geqslant 6$, the cross sections show an oscillating structure as a function of the electron energy. This behavior of the cross sections is in sharp contrast to the dramatic (by many orders of magnitude) increase in the cross section maxima with increasing v_i where the DEA process proceeds through the X $^2\Sigma_g^+$ shape resonance, where no oscillatory structures are observed [1]. The difference in the magnitude of DEA cross sections in these two cases is ascribed to the large difference in the widths of the two resonances which makes the respective entrance probabilities, corresponding to the inhomogeneous part of the nuclear wave equation, quite different. The oscillatory structure in the DEA cross sections for $v_i \geqslant 6$ in the case of Rydberg resonance is ascribed to the overlap of the vibrational wave function of the target molecule with the regular Green's function of the resonant state.

The DEA rate coefficients for all initial vibrational states of H_2, (calculated with a Maxwellian electron velocity distribution) exhibit maxima at about $T \approx 10$ eV, and demonstrate the expected T-behavior at temperatures well below and above this value. The comparison of the present rate coefficients shows that for $v_i \leqslant 2$ they are significantly larger than those when the process proceeds *via* the X $^2\Sigma_u^+$ shape resonance.

Acknowledgments

The authors thank Dr. A. Laricchiuta for providing assistance in the calculations and for useful discussions. This work has been partially supported by the ESA – ESTEC (Contract No. 21790/08/NL/HE).

References

[1] J.M. Wadehra, Appl. Phys. Lett. 35 (1979) 917.
[2] R. Celiberto, R.K. Janev, A. Laricchiuta, M. Capitelli, J.M. Wadehra, D.E. Atems, Atomic Data Nucl. Data Tables 77 (2001) 161.
[3] R.K. Janev, Contrib. Plasma Phys. 38 (1998) 307.
[4] S. Lepp, P.C. Stancil, A. Dalgarno, J. Phys. B: At. Mol. Opt. Phys. 35 (2002) R57.
[5] J.N. Bardsley, J. Phys. B (Proc. Phys. Soc.) 1 (1968) 349.

[6] D.E. Atems, J.M. Wadehra, Phys. Rev. A 42 (1990) 5201.
[7] B.I. Schneider, M. Le Dournueuf, P.G. Burke, J. Phys. E: At. Mol. Phys. 12 (1979) L365.
[8] S.A. Kalin, A.K. Kazansky, J. Phys. B: At. Mol. Opt. Phys. 23 (1990) 4377.
[9] S.A. Pozdneev, Journal of Experimental and Theoretical Physics 99 (2004) 915.
[10] W. Domcke, Phys. Rep. 208 (1991) 97.
[11] A. Chutjian, A. Garscadden, J.M. Wadehra, Phys. Rep. 264 (1996) 393.
[12] M. Čížek, J. Horáček, W. Domcke, J. Phys. B. 31 (1998) 2571.
[13] J. Comer, F.H. Read, J. Phys. B 4 (1971) 368.
[14] D.T. Stibbe, J. Tennyson, J. Phys. B 31 (1998) 815.
[15] J. Tennyson, Phys. Rep. 491 (2010) 29.
[16] D.T. Stibbe, J. Tennyson, Phys. Rev. Lett. 79 (1979) 4116.
[17] R. Celiberto, R.K. Janev, J.M. Wadehra, A. Laricchiuta, Phys. Rev. A 77 (2008) 012714.
[18] E.M. de Oliveira, M.A.P. Lima, Marcio T. do, N. Varella, Phys. Rev. A 78 (2008) 042704.
[19] G.J. Schulz, Phys. Rev. 113 (1959) 816.
[20] D. Rapp, T.E. Sharp, D.D. Briglia, Phys. Rev. Lett. 14 (1965) 533.
[21] G.J. Schulz, Rev. Mod. Phys. 45 (1973) 378.
[22] J.M. Wadehra, in: M. Capitelli (Ed.), Non Equilibrium Vibrational Kinetics, Topics in Current Physics, vol. 39, Springer-Verlag, Berlin, 1986, p. 191.
[23] R. Celiberto, R.K. Janev, J.M. Wadehra, A. Laricchiuta, Phys. Rev. A 80 (2009) 012712.
[24] W. Kolos, L. Wolniewicz, J. Chem. Phys. 43 (1965) 2429.
[25] J.N. Bardlsey, J.M. Wadehra, Phys. Rev. A 20 (1979) 1398.
[26] L. Dubé, A. Herzenberg, Phys. Rev. A 20 (1979) 194.
[27] J. Horáček, M. Čížek, K. Houfek, P. Kolorenč, W. Domcke, Phys. Rev. A 70 (2004) 052712.
[28] A. Huetz, F. Gresteau, R.I. Hall, J. Mazeau, J. Chem. Phys. 72 (1980) 5297.
[29] J. Tennyson, J. Phys. B 20 (1987) L375.
[30] R. Celiberto, U.T. Lamanna, M. Capitelli, Phys. Rev. A 50 (1994) 4778.
[31] J. Horáček, J. Phys. A: Math. Gen. 22 (1989) 355.
[32] D. Rapp, D.D. Briglia, J. Chem. Phys. 43 (1965) 1480.
[33] T.F. O'Malley, Phys. Rev 150 (1966) 14.
[34] R. Celiberto, A. Laricchiuta, M. Capitelli, Phys. Scripta T96 (2002) 32.